Chinese Chemical Letters 33 (2022) 4912–4917

Contents lists available at ScienceDirect

Chinese Chemical Letters

journal homepage: www.elsevier.com/locate/cclet

A bio-based epoxy resin derived from *p*-hydroxycinnamic acid with high mechanical properties and flame retardancy

Xin Song, Ze-Peng Deng, Chun-Bo Li, Fei Song*, Xiu-Li Wang, Li Chen, De-Ming Guo, Yu-Zhong Wang*

The Collaborative Innovation Center for Eco-Friendly and Fire-Safety Polymeric Materials (MoE), National Engineering Laboratory of Eco-Friendly Polymeric Materials (Sichuan), State Key Laboratory of Polymer Materials Engineering, College of Chemistry, Sichuan University, Chengdu 610064, China

ARTICLE INFO

Article history:
Received 26 November 2021
Revised 22 December 2021
Accepted 23 December 2021
Available online 29 December 2021

Keywords:
Epoxy resin
Bio-based
p-Hydroxycinnamic acid
Mechanical performance
Intrinsic flame retardancy

ABSTRACT

Recent advances in epoxy resins have been forward to achieving high mechanical performance, thermal stability, and flame retardancy. However, seeking sustainable bio-based epoxy precursors and avoiding introduction of additional flame-retardant agents are still of increasing demand. Here we report the synthesis of *p*-hydroxycinnamic acid-derived epoxy monomer (HCA-EP) *via* a simple one-step reaction, and the HCA-EP can be cured with 4,4′-diaminodiphenylmethane (DDM) to prepare epoxy resins. Compared with the typical petroleum-based epoxy resin, bisphenol A epoxy resin, the HCA-EP-DDM shows a relatively high glass transition temperature (192.9 °C) and impressive mechanical properties (tensile strength of 98.3 MPa and flexural strength of 158.9 MPa). Furthermore, the HCA-EP-DDM passes the V-1 flammability rating in UL-94 test and presents the limiting oxygen index of 32.6%. Notably, its char yield is as high as 31.6% under N_2, and the peak heat rate release is 60% lower than that of bisphenol A epoxy resin. Such findings provide a simple way of using *p*-hydroxycinnamic acid instead of bisphenol A to construct high-performance bio-based thermosets.

Epoxy resins are one of the most important thermosets that have been widely used for coatings, adhesives, and electronic packaging due to outstanding mechanical properties, dimensional stability, chemical resistance, adhesion, and electrical insulation. Nowadays, most commercialized epoxy resins are still developed from diglycidyl ether of bisphenol A (DGEBA) [1]. DGEBA can be synthesized by using epichlorohydrin (ECH) and bisphenol A (BPA). ECH has been produced from bio-based glycerol [2], however, BPA can be merely synthesized from non-renewable chemicals. More seriously, BPA has been acknowledged as an endocrine disruptor and reprotoxic substance [3–5]; this makes restriction of the application of DGEBA in food contact materials [6]. Hence, recent interests have been particularly gained for seeking sustainable and safe alternatives to replace DGEBA.

During the past decade, some biomass feedstocks have been explored to prepare bio-based epoxy resin with high glass transition temperature (T_g) and mechanical properties [7–14]. For example, Wan *et al.* [7] reported a bio-based epoxy resin prepared from eugenol and 4,4′-diaminodiphenyl sulfone. The cured epoxy resin showed a high T_g of 207 °C. Liu *et al.* [9] synthesized a bio-based epoxy monomer based on vanillin and guaiacol. The obtained epoxy resin exhibited a higher T_g of 187 °C and higher tensile strength, as compared to that of DGEBA-based epoxy resin. Xu *et al.* [11] used vanillin to prepare a bio-based epoxy monomer, which was cured with 4,4′-diaminodiphenylmethane (DDM) to prepare an epoxy resin with a high T_g of 206 °C and high tensile strength of 122 MPa. Fache *et al.* [12] prepared a new vanillin-derived diepoxy monomer and the cured epoxy resin showed a comparable T_g and higher storage modulus than that of DGEBA-based epoxy resin.

Despite the remarkable progress in bio-based epoxy resins, the shortages of high flammability, similar to petroleum-based ones, are still difficult to overcome. This greatly limits their applications with strong requirement of fire safety [15]. Recently, regarding the concerns on environmental and human health, halogen-free flame-retardants generally containing phosphorus [16], silicon [17], or other halogen-free flame-retardant elements [18,19] have attracted much attention. Although exhibiting satisfactory flame retardant effects, the poor compatibility of these flame retardants with substrates is still the main obstacle that inevitably deteriorates mechanical performances of resulting epoxy resins [20]. Developing epoxy resins with intrinsic flame retardancy has therefore become a trend to resolve the contradictions. Many researchers

* Corresponding authors.
E-mail addresses: songfei520@gmail.com (F. Song), yzwang@scu.edu.cn (Y.-Z. Wang).

https://doi.org/10.1016/j.cclet.2021.12.067
1001-8417/

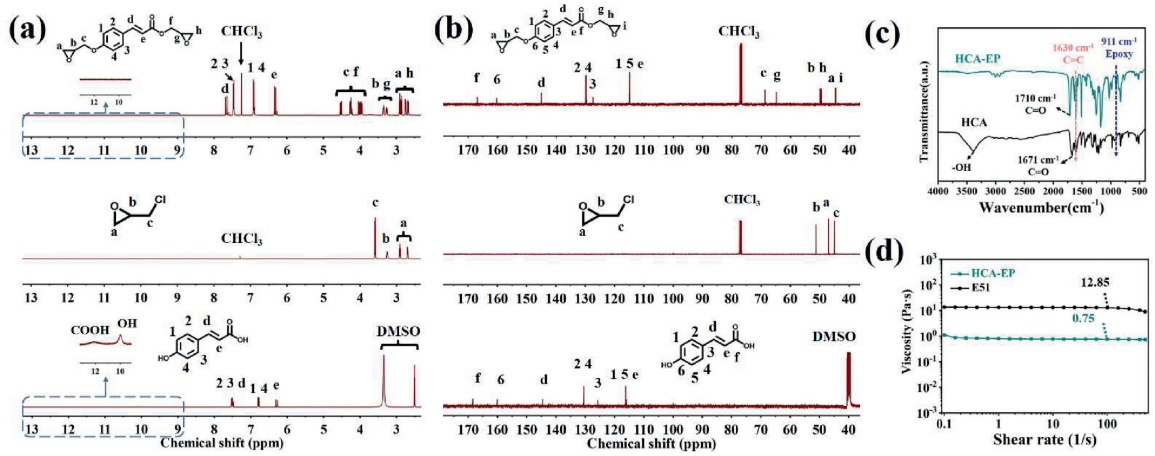

Fig. 1. (a) ^{1}H NMR and (b) ^{13}C NMR spectra of HCA, ECH and HCA-EP. (c) FTIR spectra of HCA and HCA-EP. (d) Viscosity of HCA-EP and E51 determined from 0.1 s^{-1} to 500 s^{-1} at 25 °C.

have prepared bio-based epoxy resins with good intrinsic flame retardancy by using different curing agents [21–23]. Particularly, DDM is considered as one of the most common curing agents because of low price and good overall performance. Up to now, many researchers have prepared bio-based epoxy resins cured by DDM with good flame retardancy [24–30]. Qi *et al.* [26] designed a bio-based monomer with aromatic *N*-heterocycle. After curing with DDM, the resulting epoxy resin showed a T_g of 187 °C and peak of heat rate release (PHRR) of 184.5 W/g. Similarly, Liu *et al.* [30] synthesized a bio-based epoxy monomer containing 9,10-dihydro-9-oxa-10-phosphaphenanthrene-10-oxide unit from vanillin and guaiacol, with which the prepared epoxy resin exhibited a T_g (176.4 °C) and preferable flame retardancy with a PHRR around 300 W/g. However, the tensile and flexural strengths of the epoxy resins are relatively low compared with that of DGEBA-based epoxy resin. Dai *et al.* [27] used renewable genistein to synthesize an epoxy monomer and found that the obtained epoxy resins had high mechanical properties. Nevertheless, a limited reduction in the PHRR, as compared with DGEBA-DDM, was realized. Hence, it remains necessary but challenging to develop bio-based epoxy resins with balanced high intrinsic flame retardancy and mechanical properties.

Here, considering the positive contribution of rigid conjugate structure to char forming capacity, we propose to synthesize a new bio-based epoxy monomer (Scheme 1), for the first time, from p-hydroxycinnamic acid (HCA) that widely exists in various vegetables and fruits, such as carrot, tomato, strawberry, and pineapple. The curing of epoxy monomer with DDM is conducted, as compared with the DGEBA epoxy counterpart. After curing, the thermomechanical and mechanical properties, thermal stability and flame retardancy of the resulting epoxy resin are investigated, and corresponding flame retardant mechanism is disclosed.

HCA-EP is synthesized by using ECH to react with the hydroxy and carboxyl groups of HCA (Scheme 1). Chemical structures of HCA, ECH and HCA-EP are characterized by ^{1}H NMR, ^{13}C NMR and FTIR measurements (Fig. 1). The characteristic proton peaks at 11.96 and 9.99 ppm attributing to the hydroxyl and carboxyl groups of HCA are not observed in the ^{1}H NMR spectrum of HCA-EP; the characteristic proton peaks (2.68, 2.75, 2.88, 3.27 and 3.35 ppm) of ^{1}H NMR and carbon peaks (49.96, 49.53, 44.73 and 44.62 ppm) of ^{13}C NMR spectra belonging to the epoxy group of HCA-EP are detected. Furthermore, the HCA-EP presents no characteristic peaks of ECH in the ^{1}H NMR and ^{13}C NMR spectra. The chemical shifts of H and C atoms in the spectra are in accordance with the theoretical values of the HCA-EP structure. Besides, from the FTIR spectra,

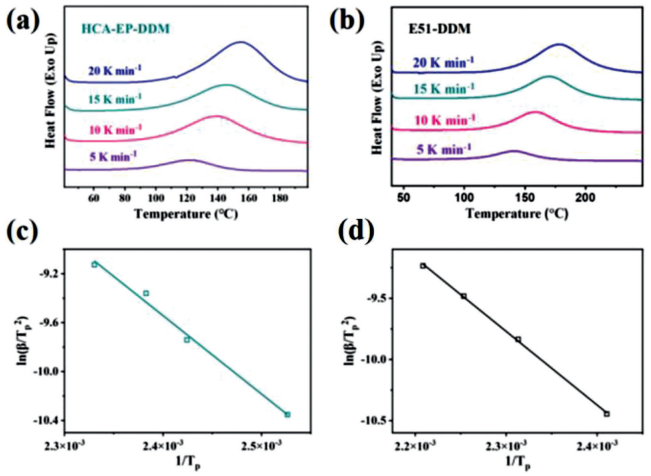

Fig. 2. Non-isothermal curves obtained from DSC (a) HCA-EP-DDM and (b) E51-DDM *via* heating rates of 5, 10, 15 and 20 °C/min. Linear fitting curves of ln (β/T_p^2) *versus* $1/T_p$ according to Kissinger's equation for (c) HCA-EP-DDM and (d) E51-DDM curing systems.

a characteristic absorption peak attributing to epoxy group [31] is observed at 911 cm^{-1}, while the peak around 1630 cm^{-1}, corresponding to CH=CH [32] is detected. The results suggest the successful introduction of epoxy group as well as the maintenance of vinyl group for HCA. It should be noted that, moreover, HCA-EP has a much lower viscosity than that of E51 (one of the most important representative commercialized epoxy resins [29]) at a shear rate of 0.1–100 s^{-1}, indicating a good processibility for further preparation of epoxy resin

The curing behaviors of HCA-EP-DDM and E51-DDM are further investigated in terms of non-isothermal curing kinetics at different heating rates (Fig. 2). With the increase of heating rate, the curing exothermic peak temperature (T_p) shifts to the high-temperature direction, mainly due to a greater thermal effect but less time for tracking the curing behavior. Additionally, the HCA-EP-DDM system presents a lower T_p compared with E51-DDM, which is possibly attributed to a higher epoxy value of HCA-EP. To compare the curing activities of two curing systems, Kissinger's method [33] is used for calculating the activation energy (E_a).

$$\ln\left(\frac{\beta}{T_p^2}\right)=\ln\left(\frac{AR}{E_a}\right)-\frac{E_a}{RT_p} \quad (1)$$

Table 1
E' at 30 °C, T_g, E_r and v_e obtained by DMA.

Sample	*E'* (10^3 MPa) at 30 °C [a]	T_g (°C) [b]	E_r (MPa) [c]	v_e (10^3 mol/m^3) [d]
HCA-EP-DDM	3.21	192.9	37.52	3.23
E51-DDM	2.22	178.8	29.17	2.59

[a] *E'* (10^3 MPa) at 30 °C: *G'* at 30 °C;
[b] T_g: The peak temperature of the curve for tanδ;
[c] E_r: *G'* in the rubbery plateau region;
[d] v_e: Crosslinking density.

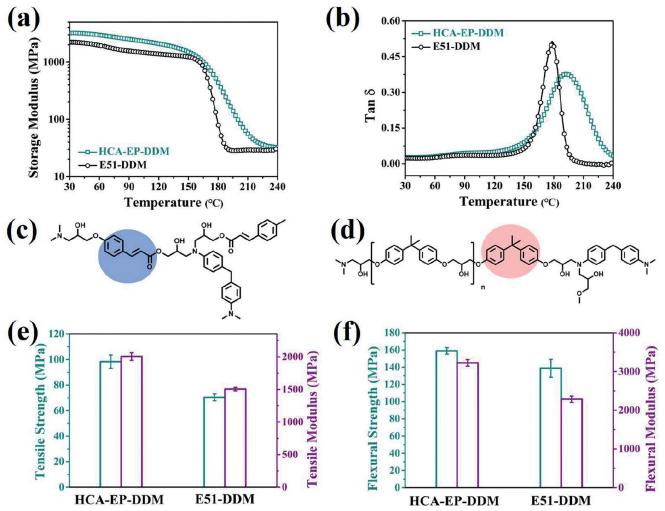

Fig. 3. The curves of (a) storage modulus (*G'*) and (b) tanδ *versus* temperature for HCA-EP-DDM and E51-DDM obtained by DMA. The structure of crosslinking networks for (c) HCA-EP-DDM and (d) E51-DDM. (e) Tensile strength and Young's modulus from tensile test and (f) flexural strength and modulus from flexural test of HCA-EP-DDM and E51-DDM.

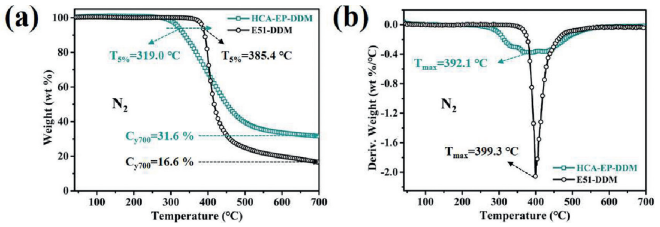

Fig. 4. (a) TGA and (b) DTG curves of HCA-EP-DDM and E51-DDM under N_2 atmosphere.

where β is the heating rate, T_p is the exothermic peak temperature, E_a is the activation energy of the curing reaction, R is the gas constant (8.314 J mol^{-1} K^{-1}), and A is the pre-exponential factor. The detailed data, including T_p and E_a of the two systems, are shown in Table S1 (Supporting information). The E_a of HCA-EP-DDM is comparable to that of E51-DDM, suggesting their similar curing behaviors. Furthermore, the curing of the HCA-EP-DDM system is determined by recording the FTIR spectra. As shown in Fig. S1 (Supporting information), characteristic absorption of epoxy group at 911 cm^{-1} disappears while the characteristic band at 1630 cm^{-1} corresponding to CH=CH still exists after the treatment; the results indicate the curing reaction occurs on the oxirane ring rather than the double carbon bond.

Fig. 3 shows storage modulus (*G'*) and loss factor (tanδ) of HCA-EP-DDM and E51-DDM as a function of temperature. The corresponding *G'* at 30 °C (*E'* at 30 °C), T_g, *G'* in the rubbery plateau region (E_r) and crosslinking density (v_e) are demonstrated in Table 1. The *E'* at 30 °C and T_g of HCA-EP-DDM are 3.21×10^3 MPa and 192.9 °C, which are higher than those of E51-DDM (2.22×10^3 MPa and 178.8 °C). According to previous reports [24], *G'* and T_g are relevant to segmental mobility and v_e. The conjugate structure (π-π structure of phenylethylene) of HCA-EP-DDM tends to preferably restrict the segmental mobility, as compared with the bisphenol A structure of E51-DDM (Figs. 3c and d) [34]. Besides, v_e can be calculated from the plateau of the elastic modus in the rubbery state according to Eq. S1 (Supporting information) [24]. The v_e of cured HCA-EP-DDM and E51-DDM is calculated to be 3.23×10^3 mol/m^3 and 2.59×10^3 mol/m^3, respectively; this can be explained by that a higher epoxy value may form a higher-crosslinking network (a higher v_e) [28]. Mechanical properties of cured epoxy resins are studied using the tensile and flexural measurements (Fig. 3 and Table S2 in Supporting information). The tensile and flexural strengths of HCA-EP-DDM are 98.3 and 158.9 MPa, which are higher than those of E51-DDM (70.3 and 138.8 MPa). Moreover, HCA-EP-DDM exhibits 32% and 41% higher Young's and flexural modulus (2.00×10^3 MPa and 3.22×10^3 MPa) than those of E51-DDM (1.51×10^3 and 2.29×10^3 MPa). As reported before [25], mechanical strength and modulus depends closely on the molecular rigidity and crosslinking density. Internal rotation is difficult to occur for conjugate structure of benzene ring and double bond, thus HCA-EP-DDM with the conjugated π-π structure and high v_e presents stronger mechanical performances over E51-DDM.

The TGA and differential thermogravimetry (DTG) curves of HCA-EP-DDM and E51-DDM under N_2 atmosphere are shown in Fig. 4. The corresponding data, including the temperature where 5 wt% weight is lost ($T_{5\%}$), maximum weight loss temperature (T_{max}) and the residual weight at 700 °C (C_{y700}), are marked. Under N_2 atmosphere, E51-DDM shows a single-step degradation process, presenting the $T_{5\%}$ of 385.4 °C and T_{max} of 399.3 °C. A high maximum degradation rate of 2.07 wt%/°C is detected within 380 to 550 °C. Similarly, HCA-EP-DDM also presents a one-step degradation process under N_2 atmosphere. HCA-EP-DDM exhibits the $T_{5\%}$ of 319.0 °C and T_{max} of 392.1 °C. The lower $T_{5\%}$ of HCA-EP-DDM can be explained by the easy fracture of the unsaturated C=C double bond as well as the C–C single bond between benzene ring and double bond [25]. However, its thermostability still meets the requirement for electrical epoxy resins according to the standard IPC-TM-650. In addition, it should be noted that, the maximum degradation rate of HCA-EP-DDM is 0.38 wt%/°C, which is 82% lower than that of E51-DDM, indicating that HCA-EP-DDM has gentle thermal degradation performance. Besides, HCA-EP-DDM exhibits a much higher char residue amount of 31.6% than that of E51-DDM (16.6%); this can be due to the high cross-linking density and the presence of conjugate structure (π-π structure of phenylethylene) that provide stronger carbonization [21,35]. Thermal stability of cured epoxy resins under air atmosphere is shown in Fig. S2 (Supporting information). Different from the results under N_2 atmosphere, both HCA-EP-DDM and E51-DDM present two-stage degradation. For the first degradation process, HCA-EP-DDM shows a lower $T_{5\%}$ and T_{max1} than those of E51-DDM, due to the presence of C=C double bond and C–C single bond between benzene ring and double bond which accounts for the similar behaviors under N_2 atmosphere [25]. However, the maximum degradation rate of

Table 2
LOI and UL-94 rating of HCA-EP-DDM and E51-DDM.

Samples	UL-94			LOI
	t_1	t_2	Rating	
HCA-EP-DDM	4.5 s	6.5 s	V1	32.6%
E51-DDM	>30 s	NA	NR	26.5%

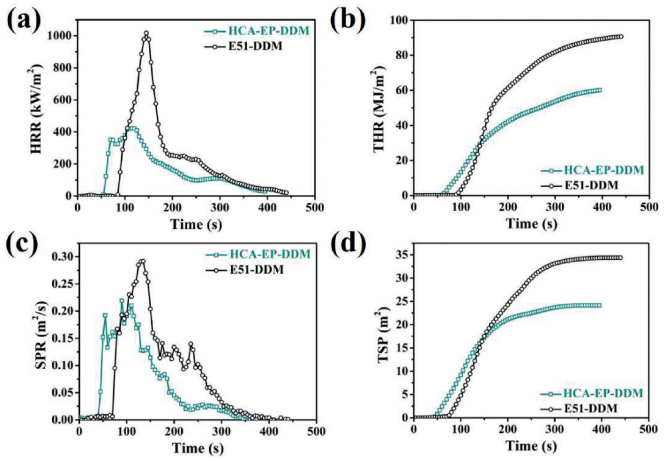

Fig. 5. (a) HRR, (b) THR, (c) SPR and (d) TSP curves of HCA-EP-DDM and E51-DDM tested by cone calorimeter test.

HCA-EP-DDM is only 0.27 wt%/°C, which is 90% lower than that of E51-DDM (2.75 wt%/°C). In the second step, HCA-EP-DDM shows a T_{max2} of 601.9 °C, which is close to that of E51-DDM (606.0 °C). Besides, the char residue amount of HCA-EP-DDM is higher than that of E51-DDM above 403.7 °C, indicating HCA-EP-DDM possesses stronger carbonization performance. A possible decomposition process of HCA-EP-DDM under air atmosphere is summarized: (1) Sluggish degradation from 300 to 520 °C corresponding to the first degradation process with formation of some char layers; (2) The oxidized decomposition of unstable char layer.

The flame retardance of cured epoxy resins is investigated with limiting oxygen index (LOI), vertical burning (UL-94) and cone calorimeter measurements. As shown in Fig. S3 (Supporting information) and Table 2, E51-DDM presents a UL-94 rating of NR and LOI of 26.5%. In contrast, HCA-EP-DDM shows stronger flame resistance with a UL-94 rating of V1 and LOI of 32.6%. Fig. 5 exhibits the curves of heat release rate (HRR), total heat release (THR), smoke production release (SPR) and total smoke production (TSP) of cured epoxy resins. The corresponding data, including time to ignition (TTI), THR, the peak of heat release rate (PHRR), calculated fire growth rate (FIGRA), TSP and char residue yield are shown in Table S3 (Supporting information). The TTI of HCA-EP-DDM is lower than that of E51-DDM, which is in accordance with the TGA result. HCA-EP-DDM exhibits a PHRR of 437 kW/m^2, with an obvious reduction of 60% compared with that of E51-DDM (1088 kW/m^2). Similarly, the THR and TSP of HCA-EP-DDM is reduced by 34% and 30%, respectively, compared with those of E51-DDM. Besides, based on the HRR curves, FIGRA of HCA-EP-DDM is relatively low, indicating HCA-EP-DDM has higher fire safety. The char residue amount of HCA-EP-DDM after combustion is 29.7 wt%, which is much higher than that of E51-DDM (7.3 wt%). Therefore, it can be concluded that HCA-EP-DDM exhibits a high flame retardance with a UL-94 rating of V1, LOI of 32.6%, and PHHR as low as 437 kW/m^2.

To understand the flame retardant mechanism of HCA-EP-DDM, SEM, Raman, XPS and TG-FTIR measurements are conducted. As shown in Fig. 6, E51-DDM cannot retain its original structure

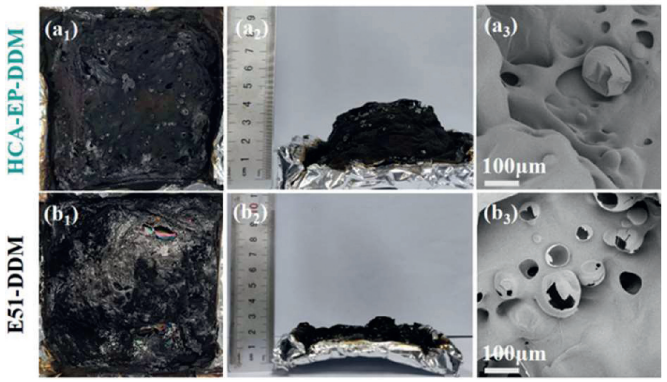

Fig. 6. Digital photos and SEM morphologies of char residues after cone calorimeter test for (a_1–a_3) HCA-EP-DDM and (b_1–b_3) E51-DDM.

but shows fragile and discrete char residue; in contrast, HCA-EP-DDM maintains the shape with consecutive and intumescent char residues. From the Raman results shown in Fig. 7, two characteristic peaks at 1350 cm^{-1} (corresponding to D bond) and 1590 cm^{-1} (corresponding to G bond) are detected for cured epoxy resins after burning. The ratio of D and G bonds (I_D/I_G) represents the degree of graphitization. A lower I_D/I_G means a more regular structure. The I_D/I_G of HCA-EP-DDM (2.65) is lower than that of E51-DDM, indicating that HCA-EP-DDM forms more regular char layer during combustion. From the XPS survey for the char residues after cone calorimeter test (Fig. 8 and Fig. S4 in Supporting information), both HCA-EP-DDM and E51-DDM have three characteristic peaks of C 1s and N 1s. For the C 1s spectrum, peaks at 284.6, 285.2 and 288.9 eV are associated with C–C, C–N and C=C/C=N bonds [36]; for the N 1s spectrum, peaks at 398.5, 400.3 and 403.2 eV are attributed to pyridine, pyrrole and pyridine-N-oxide [37]. As reported before [38], the pyridine structure is more stable than the pyrrole structure, benefitting for forming stable char layer. The above results indicate that HCA-EP-DDM possesses more stable char residues after burning due to formation of more pyridine (Table S4 in Supporting information). From the 3D TG-FTIR results shown in Figs. 9a and b, the gas phase products are determined for HCA-EP-DDM and E51-DDM during the total thermal-degradation process. HCA-EP-DDM shows lower absorbance than that of E51-DDM, indicating less gaseous products formed from HCA-EP-DDM. Figs. 9c and d exhibits the FTIR spectra of the gaseous products at the maximum decomposition rate, from which CO_2 (2358 cm^{-1} and 2309 cm^{-1}) and NH_3 (3800–3700 cm^{-1}) [25] are detected for the HCA-EP-DDM system while aromatic alcohols (3651 cm^{-1}), hydrocarbons (3140–2650 cm^{-1}), aromatic compounds (1611 cm^{-1} and 1511 cm^{-1}) [25,35,39] are observed for the E51-DDM system. The results indicate the breakage of backbone of E51-DDM during thermal-degradation process, generating flammable aromatic compounds, thus causing poor charring ability and promoted combustion. In comparison, the gaseous products of HCA-EP-DDM contain much less flammable gasses as well as more nonflammable CO_2 and NH_3. Besides, aromatic compounds and aromatic alcohols are hardly detected in the gaseous products of HCA-EP-DDM, indicating the well preservation of aromatic compounds in the condensed phase that contributes to forming stable char residues. Thus, based on the SEM, Raman, XPS and TG-FTIR results, HCA-EP-DDM follows both synergic condensed-phase and gaseous-phase flame retardant mechanism. For the condensed phase, the presence of conjugate structure and high crosslinking density enhances the formation of char residues as a protective layer to block oxygen and heat. For the gaseous phase, mainly nonflammable gasses (CO_2 and NH_3) are released, which could take away the heat and dilute the flammable gaseous products.

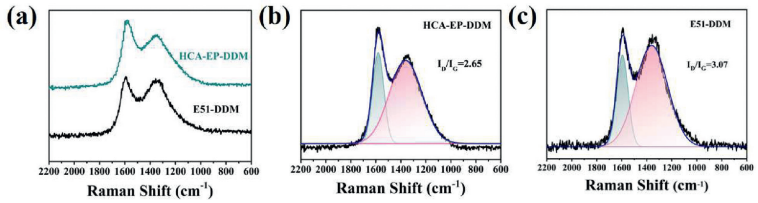

Fig. 7. Raman spectra of char residues for (a) full survey; peak splitting for (b) HCA-EP-DDM and (c) E51-DDM after cone calorimeter test.

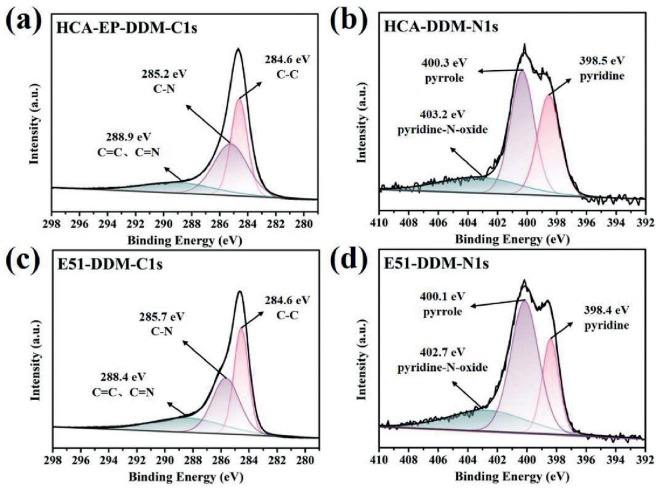

Fig. 8. The high-resolution XPS spectra for (a, c) C 1s and (b, d) N 1s for char residues of HCA-EP-DDM and E51-DDM after cone calorimeter test.

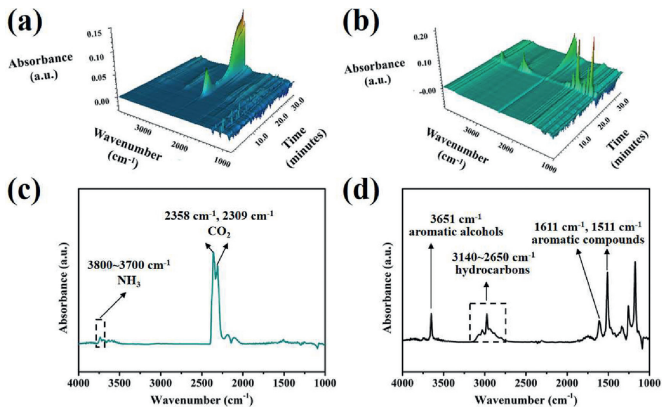

Fig. 9. The 3D TG-IR spectra of the gas phase products during the total thermal degradation process for (a) HCA-EP-DDM and (b) E51-DDM. The FTIR spectra of the gaseous products at temperature of the maximum decomposition rate of (c) HCA-EP-DDM and (d) E51-DDM.

As we know, high mechanical properties, T_g and flame retardance should be particularly noted for epoxy resins. Thus, tensile strength, flexural strength, T_g and PHRR (%) (decrease percentage of PHRR compared with E51-DDM) of recently reported bio-based epoxy resins cured with DDM are summarized in Fig. 10 [24–30]. Our work exhibits relatively high comprehensive performances among bio-based epoxy resins. Specifically, HCA-EP-DDM exhibits a relatively high PHRR (%) in this work, indicating high flame retardancy among relevant works. Furthermore, the mechanical properties (tensile and flexural strengths) and T_g of HCA-EP-DDM are comparable to or even higher than the bio-based epoxy resin counterparts.

In conclusion, we synthesized a bio-based epoxy monomer (HCA-EP) derived from *p*-hydroxycinnamic acid. The obtained

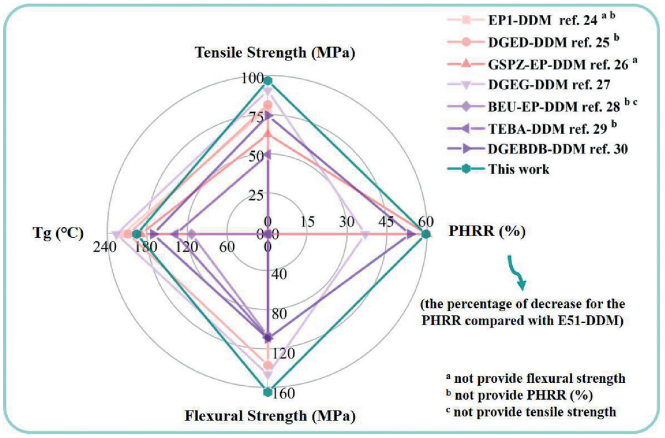

Fig. 10. Performance comparison of mechanical properties, T_g and PHRR (%) data for different bio-based epoxy resins cured by DDM.

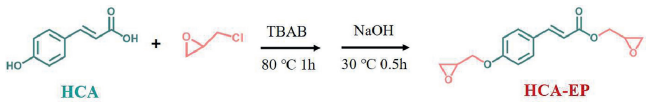

Scheme 1. Synthesis route of HCA-EP.

biomass-carbon-containing aromatic compound can be used to prepare high-performance epoxy resin with DDM as a curing agent. The HCA-EP-DDM system has higher curing reactivity and processability, because of the much low viscosity of HCA-EP as low as 0.75 Pa s (25 °C), as compared to that of a widely used precursor (E51, 12.85 Pa s). After curing, HCA-EP-DDM presents a higher T_g (192.9 °C) than that of E51-DDM. Additionally, the cured HCA-EP-DDM displays high mechanical properties with the tensile strength of 98.3 MPa and flexural strength of 158.9 MPa. Particularly, the HCA-EP-DDM system exhibits a high char yield of 31.6% (in N_2), a peak heat rate release (PHRR) as low as 437 kW/m^2, a high limiting oxygen index (LOI) of 32.6% as well as passes the flammability rating of V-1. These results offer the bio-based epoxy monomer great potential for developing sustainable epoxy resins with high mechanical and flame retardant performance to replace toxic petroleum-derived DGEBA counterparts.

Declaration of competing interest

The authors declare no competing financial interest.

Acknowledgments

This work was supported by National Natural Science Foundation of China (Nos. 52073189 and 51822304), Science and Technology Fund for Distinguish Young Scholars of Sichuan Province (No. 2019JDJQ0025), State Key Laboratory of Polymer Materials Engineering (No. sklpme2020-3-09), and the Fundamental Research Funds for the Central Universities.

Supplementary materials

Supplementary material associated with this article can be found, in the online version, at doi:10.1016/j.cclet.2021.12.067.

References

[1] L.L. Hia, E.S. Chan, S.P. Chai, P. Pasbakhsh, J. Mater. Chem. A 6 (2018) 8470–8478.
[2] D. Cespi, R. Cucciniello, M. Ricciardi, et al., Green Chem. 18 (2016) 4559–4570.
[3] R.W. Stahlhut, W.V. Welshons, S.H. Swan, et al., Environ. Health Perspect. 117 (2009) 784–789.
[4] P. Roy, H. Salminen, P. Koskimies, et al., J. Sreroid Biochem. 88 (2004) 157–166.
[5] R. Urbatzka, A.V. Cauwenberge, S. Maggioni, et al., Chemosphere 67 (2007) 1080–1087.
[6] Q.X. Zhang, M. Molenda, T.M. Reineke, Macromolecules 49 (2016) 8397–8406.
[7] J.T. Wan, J.Q. Zhao, B. Gan, et al., ACS Sustain. Chem. Eng. 4 (2016) 2869–2880.
[8] C. Li, H. Fan, T. Aziz, et al., ACS Sustain. Chem. Eng. 6 (2018) 8856–8867.
[9] T. Liu, C. Hao, S. Zhang, et al., Macromolecules 51 (2018) 5577–5585.
[10] X.W. Xu, S.Q. Ma, J.H. Wu, et al., J. Mater. Chem. A 7 (2019) 15420–15431.
[11] X.W. Xu, S.Q. Ma, J.H. Wu, et al., J. Mater. Chem. A 8 (2020) 11261–11274.
[12] M. Fache, R. Auvergne, B. Boutevin, S. Caillol, Eur. Polym. J. 67 (2015) 527–538.
[13] Y. Ecochard, M. Decostanzi, C. Negrell, R. Sonnier, S. Caillol, Molecules 24 (2019) 1818.
[14] J.T. Miao, L. Yuan, Q.B. Guan, G.Z. Liang, A.J. Gu, ACS Sustain. Chem. Eng. 5 (2017) 7003–7011.
[15] A. Toldy, P. Anna, I. Csontos, A. Szabó, G. Marosi, Polym. Degrad. Stab. 92 (2007) 2223–2230.
[16] J.Y. Yang, Y. Xia, J. Zhao, et al., Chin. J. Polym. Sci. 38 (2020) 1294–1304.
[17] Z.P. Cheng, M.H. Fang, X.X. Chen, et al., ACS Omega 5 (2020) 4200–4212.
[18] X. Zhou, X.W. Mu, W. Cai, et al., ACS Appl. Mater. Interfaces 11 (2019) 41736–41749.
[19] H. Zhang, J. Mao, M. Li, et al., Compos. Part A Appl. Sci. Manuf. 130 (2020) 105751.
[20] L. Chen, C. Ruan, R. Yang, Y.Z. Wang, Polym. Chem. 5 (2014) 3737–3749.
[21] Y. Tian, Q. Wang, L. Shen, et al., Chem. Eng. J. 383 (2020) 123124.
[22] J.J. Meng, Y.S. Zeng, P.F. Chen, Macromol. Mater. Eng. 305 (2019) 1900587.
[23] T.Y. Gao, F.D. Wang, Y. Xu, et al., Chem. Eng. J. 428 (2022) 131173.
[24] S. Wang, S.Q. Ma, C.X. Xu, et al., Macromolecules 50 (2017) 1892–1901.
[25] J.Y. Dai, Y.Y. Peng, N. Teng, et al., ACS Sustain. Chem. Eng. 6 (2018) 7589–7599.
[26] Y. Qi, J.Y. Wang, Y. Kou, et al., Nat. Commun. 10 (2019) 2107.
[27] J.Y. Dai, N. Teng, J.K. Liu, et al., Compos. Part B: Eng. 179 (2019) 107523.
[28] W. Xie, D.L. Tang, S.M. Liu, J.Q. Zhao, Polym. Test. 86 (2020) 106466.
[29] Z.H. Chi, Z.W. Guo, Z. Xu, et al., Polym. Degrad. Stabil. 176 (2020) 109151.
[30] J.K. Liu, J.Y. Dai, S.P. Wang, et al., Compos. Part B: Eng. 190 (2020) 107926.
[31] X.C. Tan, Q. Zou, Y.Z. Huang, et al., Ind. Eng. Chem. Res. 57 (2018) 7898–7904.
[32] S.S. Xu, Y. Han, Y. Guo, et al., Eur. Polym. J. 95 (2017) 394–405.
[33] H.E. Kissinger, Anal. Chem. 29 (1957) 1702–1706.
[34] Y.L. Liu, S.Q. Ma, Q. Li, et al., Eur. Polym. J. 135 (2020) 109881.
[35] Y. Qi, Z.H. Weng, K.W. Zhang, et al., Chem. Eng. J. 387 (2020) 124115.
[36] W.J. Liang, B. Zhao, P.H. Zhao, C.Y. Zhang, Y.Q. Liu, Polym. Degrad. Stab. 135 (2017) 140–151.
[37] Y. Qi, Z.H. Weng, Y. Kou, et al., Chem. Eng. J. 406 (2021) 126881.
[38] J.R. Pels, F. Kapteijn, J.A. Moulijn, Q. Zhu, K.M. Thomas, Carbon 33 (1995) 1641–1653.
[39] F.K. Chu, C. Ma, T. Zhang, et al., Compos. Part B: Eng. 190 (2020) 107925.